




## ORIGINAL ARTICLE

# $\omega$ -6 and $\omega$ -9 polyunsaturated fatty acids with double bonds near the carboxyl head have the highest affinity and largest effects on the cardiac $I_{Ks}$ potassium channel

Briana M. Bohannon<sup>1</sup>  | Marta E. Perez<sup>1</sup> | Sara I. Liin<sup>2</sup>  | Hans Peter Larsson<sup>1</sup> 

<sup>1</sup>Department of Physiology and Biophysics, Miller School of Medicine, University of Miami, Miami, Florida

<sup>2</sup>Department of Clinical and Experimental Medicine, Linköping University, Linköping, Sweden

## Correspondence

Hans Peter Larsson, Department of Physiology and Biophysics, Miller School of Medicine, University of Miami, Miami, FL.

Email: plarsson@med.miami.edu

## Funding information

This work was supported by NIH R01-HL131461 (to H. Peter Larsson) and by the Swedish Society for Medical Research (to Sara I. Liin).

See Editorial Commentary: Elinder, F. 2019. Alpha and omega in potassium-channel opening. *Acta Physiol.* 225, e13240.

## Abstract

**Aim:** The  $I_{Ks}$  channel is important for termination of the cardiac action potential. Hundreds of loss-of-function mutations in the  $I_{Ks}$  channel reduce the  $K^+$  current and, thereby, delay the repolarization of the action potential, causing Long QT Syndrome. Long QT predisposes individuals to Torsades de Pointes which can lead to ventricular fibrillation and sudden death. Polyunsaturated fatty acids (PUFAs) are potential therapeutics for Long QT Syndrome, as they affect  $I_{Ks}$  channels. However, it is unclear which properties of PUFAs are essential for their effects on  $I_{Ks}$  channels.

**Methods:** To understand how PUFAs influence  $I_{Ks}$  channel activity, we measured effects on  $I_{Ks}$  current by two-electrode voltage clamp while changing different properties of the hydrocarbon tail.

**Results:** There was no, or weak, correlation between the tail length or number of double bonds in the tail and the effects on or apparent binding affinity for  $I_{Ks}$  channels. However, we found a strong correlation between the positions of the double bonds relative to the head group and effects on  $I_{Ks}$  channels.

**Conclusion:** Polyunsaturated fatty acids with double bonds closer to the head group had higher apparent affinity for  $I_{Ks}$  channels and increased  $I_{Ks}$  current more; shifting the bonds further away from the head group reduced apparent binding affinity for and effects on the  $I_{Ks}$  current. Interestingly, we found that  $\omega$ -6 and  $\omega$ -9 PUFAs, with the first double bond closer to the head group, left-shifted the voltage dependence of activation the most. These results allow for informed design of new therapeutics targeting  $I_{Ks}$  channels in Long QT Syndrome.

## KEYWORDS

$I_{Ks}$ , KCNE1, KCNQ1, Kv7.1, Long QT Syndrome, polyunsaturated fatty acids

## 1 | INTRODUCTION

Excitable tissues, such as brain, heart, and muscle, express a wide variety of voltage-gated ion channels that play a

critical role in the firing and the shaping of action potentials.<sup>1</sup> Voltage-gated  $K^+$  channels (Kv channels) comprise an important family of channels that are involved in the repolarization phase of the cardiac action potential.<sup>2-8</sup> The

This is an open access article under the terms of the Creative Commons Attribution-NonCommercial-NoDerivs License, which permits use and distribution in any medium, provided the original work is properly cited, the use is non-commercial and no modifications or adaptations are made.

© 2018 The Authors. *Acta Physiologica* published by John Wiley & Sons Ltd on behalf of Scandinavian Physiological Society

Kv7.1/KCNE1 macromolecular complex, here forward referred to as the  $I_{Ks}$  channel (a slow delayed rectifier Kv channel) is important for the repolarization of the cardiac ventricular action potential. Loss-of-function mutations in the  $I_{Ks}$  channel result in a prolongation of the QT interval (the interval between ventricular depolarization and repolarization) in the electrocardiogram — a characteristic of Long QT Syndrome (LQTS).<sup>9</sup> The most common form of LQTS, LQT1 is due to mutations of the cardiac  $I_{Ks}$  channel that reduce outward  $K^+$  current. LQTS predisposes individuals to Torsades de Pointes, which can degenerate into ventricular fibrillation and lead to sudden cardiac death.<sup>10,11</sup> Polyunsaturated fatty acids (PUFAs) have been shown to reverse the loss-of-function of some LQT1 mutants in  $I_{Ks}$  channels expressed in *Xenopus laevis* oocytes and also to reverse drug-induced arrhythmia in cultured cardiomyocytes and a drug-induced prolongation of the QT interval in guinea pig hearts.<sup>12,13</sup> However, the features of these PUFAs that are necessary for the effects on the  $I_{Ks}$  channel are not fully understood. This study investigates the properties of the PUFA tail with the goal of determining what features of the PUFA tail are important for the activating effects of PUFAs on the cardiac  $I_{Ks}$  channel.

The cardiac  $I_{Ks}$  channel is composed of the Kv7.1  $\alpha$ -subunit and the auxiliary  $\beta$ -subunit KCNE1.<sup>14-16</sup> The Kv7.1  $\alpha$ -subunit contains six transmembrane (TM) spanning segments, S1-S6.<sup>17-19</sup> S1-S4 comprise the voltage-sensing domain (VSD), where the S4 segment contains several positively charged arginine residues allowing it to detect changes in membrane potential and act as the voltage sensor.<sup>20-22</sup> S5-S6 make up the pore domain (PD), which allows efflux of  $K^+$  ions when the channel is in the open conformation. Four Kv7.1  $\alpha$ -subunits come together to form a functional tetrameric channel that is voltage-dependent and  $K^+$  selective. KCNE1 has a single transmembrane spanning segment and associates with Kv7.1 in the cleft between the VSD and PD, where it is in a position to modulate the activity of the Kv7.1 channel.<sup>23-25</sup> The association of KCNE1 with Kv7.1 causes the Kv7.1 channel to activate at more positive potentials, open with slower activation kinetics, and increases the single channel conductance.<sup>14,24,26,27</sup> There are a variety of mutations in both the Kv7.1 and KCNE1 subunits that result in a LQTS phenotype and these mutations have been demonstrated to affect an array of processes including voltage sensing, channel opening/closing, and channel trafficking to the membrane.<sup>28</sup>

Current treatment options for LQTS are the prescription of  $\beta$ -blockers or the implantation of a cardiac defibrillator.<sup>29</sup> However, effective at preventing arrhythmia from causing sudden cardiac death, these treatments do not target the root cause of LQTS (ie in LQT1, defects in the cardiac

$I_{Ks}$  channel). PUFAs are naturally occurring, amphipathic molecules that contain a hydrophilic, carboxyl head, and hydrophobic hydrocarbon tail.<sup>30</sup> Early evidence from animal models suggested that PUFAs modulate the activity of voltage-gated  $Na^+$  and  $Ca^{2+}$  channels and therefore could act anti-arrhythmically at the ion channel level.<sup>31-35</sup> In our lab, we have investigated the potential therapeutic effect of PUFAs on the  $I_{Ks}$  channel and our data strongly suggest that modified PUFAs affect the cardiac  $I_{Ks}$  current by shifting the voltage dependence of activation to more negative voltages.<sup>12</sup> While it is known that PUFAs can modulate the activity of the  $I_{Ks}$  channel, it is not known which properties of these PUFAs are essential for their effect on the  $I_{Ks}$  channel.

Previous data from our lab has shown that the most common PUFA in fish oil, docosahexaenoic acid (DHA), shifts the voltage dependence of activation ( $V_{0.5}$ ) of the Kv7.1 channel to more negative voltages by an electrostatic interaction between the negatively charged DHA head group and the positively charged voltage sensor of Kv7.1,<sup>12</sup> a mechanism demonstrated in Shaker  $K^+$  channels.<sup>36,37</sup> However, when DHA is applied to the physiological  $I_{Ks}$  channel (coexpression of Kv7.1 and KCNE1), there is no effect on the  $V_{0.5}$ . Interestingly, the left-shifting effect of DHA could be restored in the  $I_{Ks}$  channel by conducting experiments at pH 9 (rather than pH 7.5).<sup>12</sup> We have further shown that the presence of KCNE1 decreases the local pH near the DHA head group, so that DHA is less likely to be negatively charged in the presence of KCNE1 at physiological pH.<sup>12</sup> By increasing the pH of the extracellular solution to pH = 9, we deprotonate the DHA head group and restore its negative charge, thereby restoring the left-shifting effects of DHA on the  $I_{Ks}$  channel.<sup>12</sup> We have also shown that PUFAs with a lower pKa, such as N-arachidonoyl taurine (N-AT) that remains negatively charged when bound to  $I_{Ks}$  channels at pH 7.5, retain the ability to shift the voltage dependence of Kv7.1 even when it is co-expressed together with KCNE1.<sup>12,13</sup> While our previous data show the importance of the PUFA head group charge for shifting the  $V_{0.5}$  of the  $I_{Ks}$  channel, little is known about the importance of PUFA tail properties for the affinity of PUFAs and the effects of PUFAs on the  $I_{Ks}$  channel. Due to the limited number of commercially available PUFAs with a permanently negatively charged head group (such as N-AT), we here tested the importance of the tail properties in PUFAs with a carboxyl head group at pH 9.0 to maintain the negative charge on the head group even in the presence of KCNE1.

Here, we report that specific properties of the hydrocarbon tail are important for the effects of PUFAs on the  $I_{Ks}$  current and the apparent binding affinity of PUFAs to the  $I_{Ks}$  channel. The length and number of double bonds in the PUFA tail do not strongly correlate with the effects of

PUFAs on  $I_{Ks}$  current or the binding affinity of PUFAs to the  $I_{Ks}$  channel. However, we find that the position of the first double bond strongly correlates with both the effect of PUFAs on  $I_{Ks}$  current and the apparent binding affinity of PUFAs for the  $I_{Ks}$  channel. PUFAs that have their first double bond close to the hydrophilic head group consistently demonstrate a larger effect on the  $I_{Ks}$  current and a higher apparent affinity for the  $I_{Ks}$  channel than PUFAs that have their first double bond further away from the PUFA head. In addition, PUFAs with a double bond close to the end of the PUFA tail ( $\omega$ -3 PUFAs) are less effective compared to PUFAs with a double bond further away from the end of the PUFA tail ( $\omega$ -6 and  $\omega$ -9 PUFAs).

## 2 | RESULTS

### 2.1 | Polyunsaturated fatty acid compounds have multiple effects on the activity of the $I_{Ks}$ channel

To determine the effect of a specific PUFA (for example, eicosatrienoic acid 5,8,11), we measured its effects on the current vs voltage relationship of the  $I_{Ks}$  channel (Figure 1A-C). The tail currents were measured after different activation voltages to generate the G-V curve from which we can determine both the shift in the  $V_{0.5}$  and the increase in  $G_{max}$  (Figure 1C) once the current has reached saturation (Figure 1D). We also measured the relative increase in  $K^+$  current ( $I/I_0$ ) at 0 mV (Figure 1C), a voltage close to the systolic plateau during a cardiac action potential. Both a shift in the  $V_{0.5}$  and an increase in the  $G_{max}$  would increase the currents at 0 mV, so by measuring the currents at 0 mV we get a rough estimate of the total expected physiologically relevant, PUFA-induced change in current during a ventricular action potential.<sup>38</sup> Lastly, we determine  $K_m$  values for  $I/I_0$ ,  $\Delta V_{0.5}$ , and  $G_{max}$  to understand how different properties (ie different tail length, double bond number and bond position) affect the apparent binding affinity of the PUFAs to the  $I_{Ks}$  channel (Figure 1E). The apparent binding affinity reported throughout the text is the  $K_m$  corresponding to the increase in  $I/I_0$ , as the apparent affinities of  $I/I_0$ ,  $\Delta V_{0.5}$ , and  $G_{max}$  are comparable.

### 2.2 | Increasing the length of the PUFA tail does not increase the effects on the $I_{Ks}$ current

We first investigate the role of the carbon tail length by applying PUFAs of varying length to *Xenopus* oocytes expressing the wild type human  $I_{Ks}$  channel. Sixteen PUFAs were tested that varied in total carbon tail length while maintaining the same (carboxyl) head group (Figure S1; Table 1). The recordings were done in solutions at pH 9.0 to ensure a negatively charged head group.<sup>12</sup>

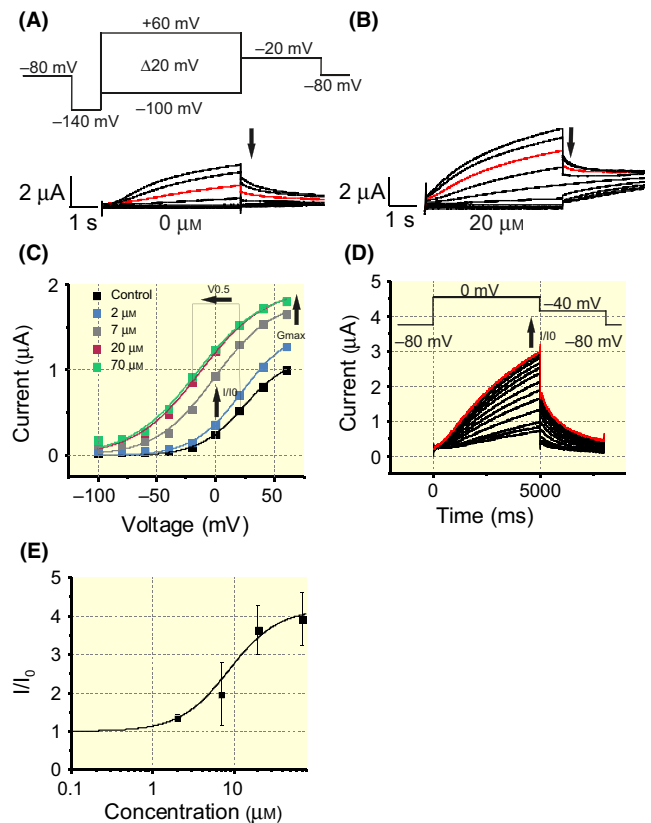


**FIGURE 1** Example of raw and analysed data from  $I_{Ks}$  recordings using 20:3 $\Delta$ 5,8,11. A,  $K^+$  current in response to increasing depolarizing voltage steps in the absence of 20:3 $\Delta$ 5,8,11 (0  $\mu$ mol/L). Red trace occurs at 20 mV (Voltage protocol shown above). B,  $K^+$  current in response to increasing depolarizing steps in the presence of 20  $\mu$ mol/L 20:3 $\Delta$ 5,8,11. C, Conductance vs voltage (G-V) relationship for series of 20:3 $\Delta$ 5,8,11 concentrations measured using  $I_{Ks}$  channel tail current (Arrow in panels A and B). D, Currents in response to a voltage step to 0 mV during application protocol. E, Dose dependent increase in relative current ( $I/I_0$ ), measured at 0 mV and fit using Equation 2

To make it easier to follow the discussion of the different PUFAs, we will refer to PUFAs using a shorthand nomenclature throughout the remainder of this paper: Carbon length: number of double bonds $\Delta$ position of double bonds. For example, the tail of DHA has 22 carbons and six double bonds at positions 4,7,10,13,16,19 where the numbering beginning at the carbonyl carbon of the PUFA head group. We will therefore call DHA 22:6 $\Delta$ 4,7,10,13,16,19.

If the length of the carbon tail is important for its effect on the  $I_{Ks}$  channel, we would expect that changing the length of the carbon tail would produce a subsequent change in  $K^+$  current amplitude. However, this is not obvious from the data. As an example, we compare four PUFAs that vary in the length of their carbon tail, but all have a carboxyl head group and have three double bonds in the same position from the end of the tail

**TABLE 1** Summary of all polyunsaturated fatty acid (PUFA) properties and effects on the  $I_{Ks}$  channel

IUPAC Name	Double bond number	Double bond positions	$\omega$	Max $I/I_0$	Max $\Delta V_{0.5}$ (mV)	Max $G_{max}/G_{max0}$	$K_m$ ( $\mu\text{mol/L}$ ) of $I/I_0$	$K_m$ ( $\mu\text{mol/L}$ ) of $\Delta V_{0.5}$	$K_m$ ( $\mu\text{mol/L}$ ) of $G_{max}$	n
Docosahexaenoic acid (4,7,10,13,16,19)	6	4,7,10,13,16,19	$\omega$ -3	3.2 ± 0.01	-20.2 ± 0.1	1.5 ± 0.2	3 ± 0.1	3.1 ± 0.1	1.8 ± 0.0	6
Docosapentaenoic acid (4,7,10,13,16)	5	4,7,10,13,16	$\omega$ -6	3.7 ± 0.02	-44.4 ± 10	1.3 ± 0.02	3.7 ± 0.07	8.8 ± 4.8	2.9 ± 0.5	3
Docosapentaenoic acid (7,10,13,16,19)	5	7,10,13,16,19	$\omega$ -3	1.6 ± 0.05	-4 ± 0.13	1.2 ± 0.01	8.72 ± 1.25	11.1 ± 0.6	1.2 ± 1.7	4
Docosatetraenoic acid (4,10,13,16)	4	4,10,13,16	$\omega$ -6	5.3 ± 0.09	-18.2 ± 0.5	2.4 ± 0.03	6.3 ± 0.27	4.4 ± 0.3	4.4 ± 0.3	3
Docosatetraenoic acid (7,10,13,16)	4	7,10,13,16	$\omega$ -6	3.3 ± 0.01	-14.9 ± 2.2	1.5 ± 0.03	11.65 ± 0.1	19.4 ± 7.3	2.7 ± 0.6	3
Docosatrienoic acid (13,16,19)	3	13,16,19	$\omega$ -3	0.69 ± 0.01	1.7 ± 0.3	1.02 ± 0.1	NA	NA	NA	4
Eicosapentaenoic acid (5,8,11,14,17)	5	5,8,11,14,17	$\omega$ -3	2.4 ± 0.05	-25 ± 4.6	1.0 ± 0.1	4.9 ± 0.49	9.8 ± 4.4	NA	3
Eicosatrienoic acid (5,8,11)	3	5,8,11	$\omega$ -9	4.0 ± 0.23	-44.7 ± 4.3	1.3 ± 0.01	9.24 ± 1.44	10.3 ± 2.2	6.0 ± 0.8	3
Eicosatrienoic acid (8,11,14)	3	8,11,14	$\omega$ -6	2.5 ± 0.04	-42.5 ± 1.9	0.95 ± 0.2	14.4 ± 2.5	16.1 ± 1.6	NA	4
Eicosatrienoic acid (11,14,17)	3	11,14,17	$\omega$ -3	1.6 ± 0.1	-4.4 ± 1.3	0.99 ± 0.1	35.2 ± 0.1	23.7 ± 7.6	NA	4
Linoleic acid (9,12)	2	9,12	$\omega$ -6	3.6 ± 0.6	-29.8 ± 1.7	1.06 ± 0.02	NA	NA	NA	3
$\alpha$ -linolenic acid (9,12,15)	3	9,12,15	$\omega$ -3	3.3 ± 0.004	-21.9 ± 0.5	1.6 ± 0.34	18.7 ± 0.05	21.9 ± 0.5	14 ± 2.4	3
$\gamma$ -linolenic acid (6,9,12)	3	6,9,12	$\omega$ -6	2.2 ± 0.1	-22.3 ± 0.5	0.9 ± 0.1	10.04 ± 0.97	12.3 ± 0.6	NA	5
Pinolenic acid (5,9,12)	3	5,9,12	$\omega$ -6	2.9 ± 0.07	-38 ± 2.7	1.1 ± 0.01	6.74 ± 0.36	10.5 ± 1.6	4.9 ± 2.2	7
Hexadecatrienoic acid (7,10,13)	3	7,10,13	$\omega$ -3	2.1 ± 0.02	-13.4 ± 0.6	0.90 ± 0.2	8.11 ± 0.21	7.2 ± 0.5	NA	4
Tetradecatrienoic acid (5,8,11)	3	5,8,11	$\omega$ -3	1.1 ± 0.15	0.80 ± 6.5	0.84 ± 0.1	NA	NA	NA	3

All values for  $I/I_0$ ,  $\Delta V_{0.5}$ ,  $G_{max}$ , and  $K_m$  for  $I/I_0$ ,  $\Delta V_{0.5}$ , and  $G_{max}$  represent the mean and standard error of the mean (SEM).

(22:3 $\Delta$ 13,16,19, 20:3 $\Delta$ 11,14,17, 18:3 $\Delta$ 9,12,15, and 16:3 $\Delta$ 7,10,13). The PUFA with the longest carbon tail (22:3 $\Delta$ 13,16,19) does not increase the maximum  $I/I_0$  ( $0.7 \pm 0.01$ ; Figure 2A), produces no change in the  $G_{\max}$  ( $1.0 \pm 0.1$ ; Figure S2), and also produces no left-shift of the  $V_{0.5}$  ( $\Delta V_{0.5} = 1.7 \pm 0.3$  mV; Figure 2B). Removing two carbons from the tail (20:3 $\Delta$ 11,14,17) increases the maximum  $I/I_0$  ( $1.6 \pm 0.1$ ; Figure 2A), but does not produce a change in the  $G_{\max}$  ( $1.0 \pm 0.1$ ; Figure S2) and produces a small shift in the  $V_{0.5}$  ( $\Delta V_{0.5} = -4.4 \pm 1.3$  mV; Figure 2B). However, shortening of the PUFA by two additional carbons (18:3 $\Delta$ 9,12,15) produces a threefold increase in maximum  $I/I_0$  ( $3.3 \pm 0.004$ ; Figure 2A), slightly increases the  $G_{\max}$  ( $1.6 \pm 0.3$ ; Figure S2), and drastically increases the left-shift of the  $V_{0.5}$  ( $\Delta V_{0.5} = -21.9 \pm 0.5$  mV; Figure 2B). In contrast, further shortening of the PUFA by two or more carbons (16:3 $\Delta$ 7,10,13), though it still produces a twofold increase in maximum  $I/I_0$  ( $2.1 \pm 0.02$ ; Figure 2A), decreases the left-shift of the  $V_{0.5}$  ( $\Delta V_{0.5} = -13.4 \pm 0.6$  mV; Figure 2B) and the change in the  $G_{\max}$  ( $0.9 \pm 0.2$ ; Figure S2). Overall, when we

compare the effects of all 16 PUFAs tested, there is no correlation between the length of the carbon tail and  $I/I_0$  (Slope =  $0.14 \pm 0.12$ ;  $R^2 = 0.09$ ;  $P = 0.26$ ; Figure 2C). There is no correlation between the length of the carbon tail and the left-shift of the  $V_{0.5}$  (Slope =  $-0.61 \pm 1.7$ ;  $R^2 = 0.01$ ;  $P = 0.72$ ; Figure 2D). There is a weak correlation between the length of the carbon tail and the maximal conductance ( $G_{\max}$ ; Slope =  $0.08 \pm 0.04$ ;  $R^2 = 0.25$ ;  $P = 0.05$ ; Figure S2B). Lastly, there is no correlation between the length of the carbon tail and the apparent binding affinity for  $I/I_0$  ( $K_m$ ; Slope =  $-0.76 \pm 1.3$ ;  $R^2 = 0.03$ ;  $P = 0.56$ ; Figure 2E).

### 2.3 | A greater number of double bonds in the PUFA tail do not increase the effects on $I_{Ks}$ current

To determine whether the number of double bonds in the tail is important for the effects of PUFAs on the  $I_{Ks}$  channel, we look next at PUFAs with different number of double bonds while the head group and the tail length are constant. We first compare two PUFAs (22:5 $\Delta$ 4,7,10,13,16 vs 22:3 $\Delta$ 13,16,19) that both have 22 carbons, but either have 5 or 3 double bonds in the tail. Decreasing the number of double bonds from 5 to 3 bonds (22:5 $\Delta$ 4,7,10,13,16 vs 22:3 $\Delta$ 13,16,19) decreases the  $I/I_0$  ( $3.7 \pm 0.02$  to  $0.7 \pm 0.01$ ; Figure 3A), removes the increase in  $G_{\max}$  ( $1.3 \pm 0.02$  to  $1.0 \pm 0.1$ ; Figure S2), and removes the left-shift of the  $\Delta V_{0.5}$  ( $\Delta V_{0.5} = -44.4 \pm 10$  mV to  $1.7 \pm 0.3$  mV; Figure 3B). In contrast, reducing the number of double bonds in PUFAs with 20-carbon tails (20:5 $\Delta$ 5,8,11,14,17 vs 20:3 $\Delta$ 5,8,11) increases the maximum  $I/I_0$  ( $2.4 \pm 0.05$  to  $4.0 \pm 0.23$ ; Figure 3A), slightly increases the  $G_{\max}$  ( $1.0 \pm 0.1$  to  $1.3 \pm 0.01$ ; Figure S2), and increases the left-shift of the  $V_{0.5}$  by a factor of 2 ( $\Delta V_{0.5} = -25 \pm 4.6$  mV to  $-44.7 \pm 4.3$  mV; Figure 3B). Overall, when we compare the effects of all 16 PUFAs tested, there is no correlation between the number of double bonds in the tail and  $I/I_0$  (Slope =  $0.16 \pm 0.29$ ;  $R^2 = 0.02$ ;  $P = 0.59$ ; Figure 3C). There is also no correlation between the number of double bonds and the shift in  $V_{0.5}$  (Slope =  $0.14 \pm 3.8$ ;  $R^2 = 0.0001$ ;  $P = 0.97$ ; Figure 3D), the  $G_{\max}$  (Figure S2C), or the apparent binding affinity of  $I/I_0$  ( $K_m$ ; Slope =  $-4.2 \pm 2.0$ ;  $R^2 = 0.28$ ;  $P = 0.06$ ; Figure 3E).

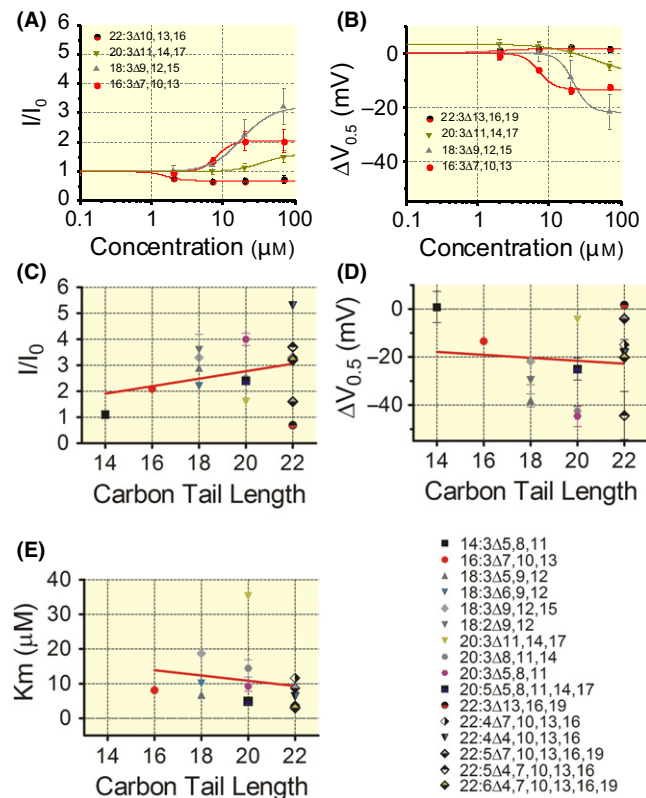


**FIGURE 2** No role of carbon tail length on polyunsaturated fatty acid (PUFA) effect and affinity. A, Dose dependent  $I/I_0$  increase in the presence of PUFAs with varying carbon tail lengths. B, Dose dependent  $\Delta V_{0.5}$ . C-E, Correlation between carbon tail length and (C)  $I/I_0$  (Slope =  $0.14 \pm 0.12$ ;  $R^2 = 0.09$ ;  $P = 0.26$ ), (D)  $\Delta V_{0.5}$  (Slope =  $-0.61 \pm 1.7$ ;  $R^2 = 0.01$ ;  $P = 0.72$ ), and (E)  $K_m$  of  $I/I_0$  (Slope =  $-0.76 \pm 1.3$ ;  $R^2 = 0.03$ ;  $P = 0.56$ )

### 2.4 | Having the first double bonds closer to head group increases apparent affinity and effect of PUFA on $I_{Ks}$ current

Because neither the tail length nor the number of double bonds in the tail correlate very strongly with the PUFA-

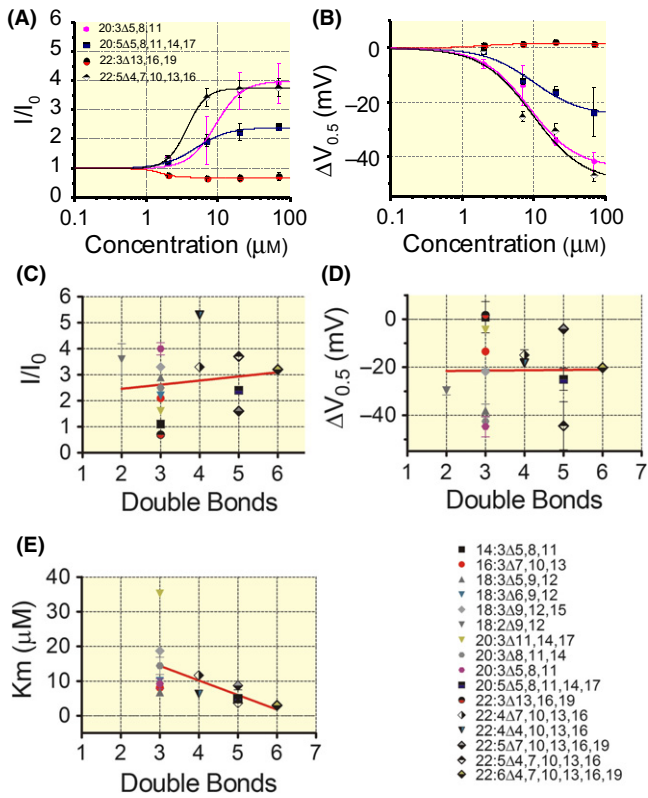


**FIGURE 3** No role of the number of double bonds on polyunsaturated fatty acids (PUFA) effect and affinity. (A), Dose dependent  $I/I_0$  increase in the presence of PUFAs with varying number of double bonds. (B), Dose dependent changes in  $\Delta V_{0.5}$ . C-E, Correlation between the number of double bonds and (C)  $I/I_0$  (Slope =  $0.16 \pm 0.29$ ;  $R^2 = 0.02$ ;  $P = 0.59$ ), (D)  $\Delta V_{0.5}$  (Slope =  $0.14 \pm 3.8$ ;  $R^2 = 0.0001$ ;  $P = 0.97$ ), and (E)  $K_m$  of  $I/I_0$  (Slope =  $-4.2 \pm 2.0$ ;  $R^2 = 0.28$ ;  $P = 0.06$ )

induced effects on the  $I_{Ks}$  channel, we investigated whether the positions of the double bonds are important for the effects of PUFAs on the  $I_{Ks}$  channel. We first compare the compounds 22:6 $\Delta$ 4,7,10,13,16,19 and 22:3 $\Delta$ 13,16,19 on the  $I_{Ks}$  channel (Figure 4A,B). Application of 22:6 $\Delta$ 4,7,10,13,16,19 produces a dose dependent increase in maximum  $I/I_0$  ( $3.2 \pm 0.1$ ; Figure 4E), produces an increase in the  $G_{max}$  ( $1.5 \pm 0.2$ ; Figure S2), and produces a significant shift in the  $V_{0.5}$  ( $\Delta V_{0.5} = -20.2 \pm 0.1$  mV; Figure 4F). However, when the first three double bonds are removed (22:3 $\Delta$ 13,16,19), there is a decrease in maximum  $I/I_0$  ( $0.7 \pm 0.01$ ; Figure 4E), no change in the  $G_{max}$  ( $1.0 \pm 0.1$ ; Figure S2), and the left-shifting effect on the  $V_{0.5}$  is abolished ( $\Delta V_{0.5} = 1.7 \pm 0.3$  mV; Figure 4F). This data show that some, or all, of the three initial double bonds in the 22:6 $\Delta$ 4,7,10,13,16,19 tail are necessary for its effects on the  $I_{Ks}$  channel. To determine whether reintroducing double bonds closer to the PUFA head improves the effects of 22:3 $\Delta$ 13,16,19, we test 22:4 $\Delta$ 7,10,13,16 and 22:4 $\Delta$ 4,10,13,16 (Figure 4C,D). 22:4 $\Delta$ 7,10,13,16

application compared to 22:4 $\Delta$ 4,10,13,16 produces a smaller increase in  $I/I_0$  ( $3.3 \pm 0.01$  and  $5.3 \pm 0.09$  respectively; Figure 4G), a smaller increase in the  $G_{max}$  ( $1.5 \pm 0.03$  and  $2.4 \pm 0.03$  respectively; Figure S2), and produces a marginally smaller shift in the  $V_{0.5}$  ( $\Delta V_{0.5} = -14.9 \pm 2.2$  mV and  $-18.2 \pm 0.5$  mV respectively; Figure 4H). In addition, positioning the first double bond closer to the head group

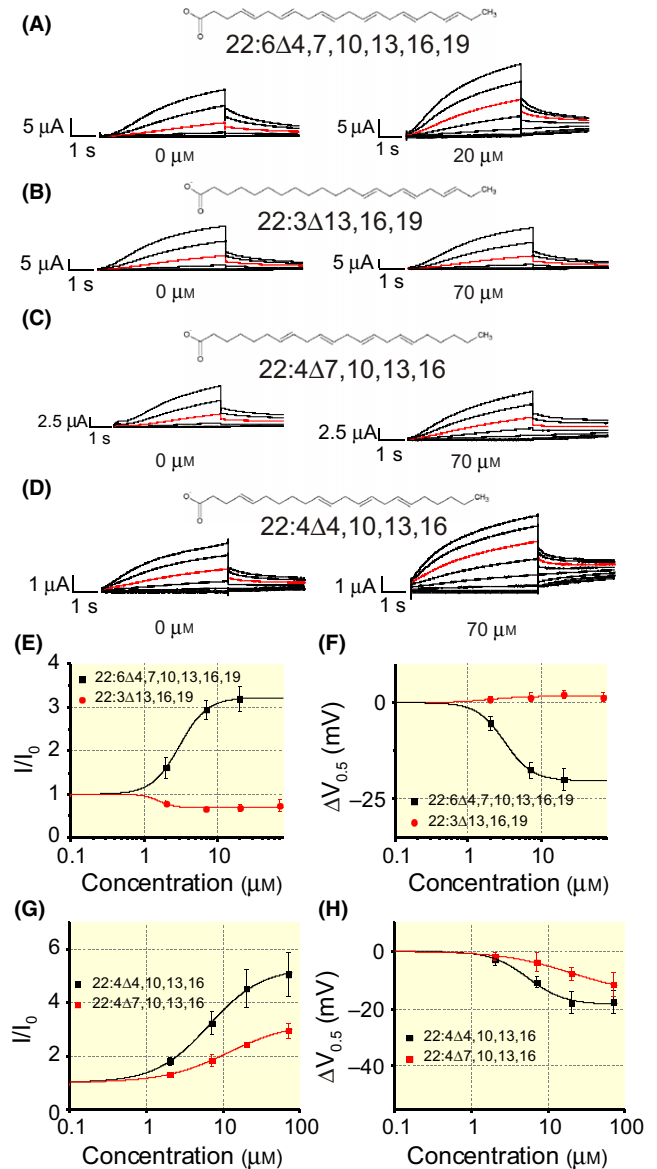


**FIGURE 4** Double bonds closer to the polyunsaturated fatty acid head rescues effect on  $I_{Ks}$  channel current and voltage shift. A,  $K^+$  current in 0  $\mu\text{mol/L}$  (Left) and 20  $\mu\text{mol/L}$  (Right) for (A) 22:6 $\Delta$ 4,7,10,13,16,19. B-D,  $K^+$  current in 0  $\mu\text{mol/L}$  (Left) and 70  $\mu\text{mol/L}$  (Right) for (B) 22:3 $\Delta$ 13,16,19, (C) 22:4 $\Delta$ 7,10,13,16, and (D) 22:4 $\Delta$ 4,10,13,16. E and G, Comparison of dose dependent  $I/I_0$  increase between (E) 22:6 $\Delta$ 4,7,10,13,16,19 and 22:3 $\Delta$ 13,16,19 and (G) 22:4 $\Delta$ 4,10,13,16 and 22:4 $\Delta$ 7,10,13,16. F and H, Comparison of dose dependent shifts in  $\Delta V_{0.5}$  of (F) 22:6 $\Delta$ 4,7,10,13,16,19 and 22:3 $\Delta$ 13,16,19, and (H) 22:4 $\Delta$ 4,10,13,16 and 22:4 $\Delta$ 7,10,13,16

increased the apparent affinity for the  $I_{K_S}$  channel, as 22:4 $\Delta$ 4,10,13,16 had a  $K_m = 6.3 \pm 0.3 \mu\text{mol/L}$ , whereas 22:4 $\Delta$ 7,10,13,16 had a  $K_m = 11.6 \pm 0.1 \mu\text{mol/L}$  (for  $I/I_0$ ;  $t$  statistic = 32.2;  $df = 4$ ;  $P < 0.0005$ ). This suggests that the location of the first double bond close to the hydrophilic head group of the PUFA is important for improving the effects on and the apparent affinity for the  $I_{K_S}$  channel.

Next, we test three 20-carbon PUFAs (20:3 $\Delta$ 5,8,11, 20:3 $\Delta$ 8,11,14, and 20:3 $\Delta$ 11,14,17) that all contain the same number of double bonds, but the double bonds start at different distances from the carboxyl head group (Figure 5A-C). 20:3 $\Delta$ 5,8,11, which has its first double bond closest in proximity to the head group, produced the largest increase in maximum  $I/I_0$  ( $4.0 \pm 0.2$ ; Figure 5D). 20:3 $\Delta$ 8,11,14, in which the double bonds are shifted further away from the head, increased the maximum  $I/I_0 < 20:3\Delta 5,8,11$  ( $2.5 \pm 0.04$ ; Figure 5D). 20:3 $\Delta$ 11,14,17, in which the double bonds are located furthest away from the PUFA head, produced the smallest increase in maximum  $I/I_0$  ( $1.6 \pm 0.1$ ; Figure 5D). 20:3 $\Delta$ 5,8,11 also slightly increased the  $G_{\text{max}}$  of the  $I_{K_S}$  channel compared to 20:3 $\Delta$ 8,11,14 and 20:3 $\Delta$ 11,14,17 ( $1.3 \pm 0.01$ ,  $1.0 \pm 0.2$  and  $1.0 \pm 0.1$  respectively; Figure 5E). 20:3 $\Delta$ 5,8,11 and 20:3 $\Delta$ 8,11,14 both produce a larger left-shift the  $V_{0.5}$  ( $\Delta V_{0.5} = -44.7 \pm 4.3 \text{ mV}$  and  $-42.5 \pm 1.9 \text{ mV}$  respectively) compared to 20:3 $\Delta$ 11,14,17 ( $-4.4 \pm 1.3 \text{ mV}$ ; Figure 5F). 20:3 $\Delta$ 5,8,11 and 20:3 $\Delta$ 8,11,14 bound to the  $I_{K_S}$  channel with comparable  $K_m$  for  $I/I_0$  ( $9.2 \pm 1.4 \mu\text{mol/L}$  and  $14.4 \pm 2.5 \mu\text{mol/L}$  respectively) and exhibited better apparent affinity for  $I/I_0$  compared to 20:3 $\Delta$ 11,14,17 ( $35.2 \pm 0.1 \mu\text{mol/L}$ ; Figure 5G). The effects and apparent affinity of 20:3 $\Delta$ 5,8,11 compared to those of 20:3 $\Delta$ 8,11,14 and 20:3 $\Delta$ 11,14,17 suggest that the location of the first double bond close to the hydrophilic head group of the PUFA is important for improving the effects on and the apparent affinity for the  $I_{K_S}$  channel.

To further test the importance of the location of double bonds relative to the head group, we compared three 18-carbon PUFAs (18:3 $\Delta$ 5,9,12, 18:3 $\Delta$ 6,9,12, and 18:3 $\Delta$ 9,12,15) that all contain the same number of double bonds, but with the double bonds at different locations (Figure 6A-C). 18:3 $\Delta$ 5,9,12 and 18:3 $\Delta$ 9,12,15 both produce the largest increases in maximum  $I/I_0$  when compared to 18:3 $\Delta$ 6,9,12 ( $2.9 \pm 0.07$  and  $3.3 \pm 0.004$  compared to  $2.2 \pm 0.06$ ; Figure 6D). Both 18:3 $\Delta$ 5,9,12 and 18:3 $\Delta$ 9,12,15 increased the  $G_{\text{max}}$  slightly ( $1.1 \pm 0.01$  and  $1.6 \pm 0.3$  respectively; Figure S2), however, 18:3 $\Delta$ 6,9,12 did not increase  $G_{\text{max}}$  ( $0.9 \pm 0.1$ ; Figure S2). 18:3 $\Delta$ 5,9,12 application resulted in the greatest left-shift in the  $V_{0.5}$  of  $I_{K_S}$  channel activation, shifting the  $V_{0.5}$  by  $-38 \pm 2.7 \text{ mV}$  (Figure 6E). In contrast, 18:3 $\Delta$ 9,12,15 and 18:3 $\Delta$ 6,9,12 both produced similar left-shifts of the  $V_{0.5}$  ( $\Delta V_{0.5} = -21.9 \pm 0.5 \text{ mV}$  and  $-22.3 \pm 0.5 \text{ mV}$

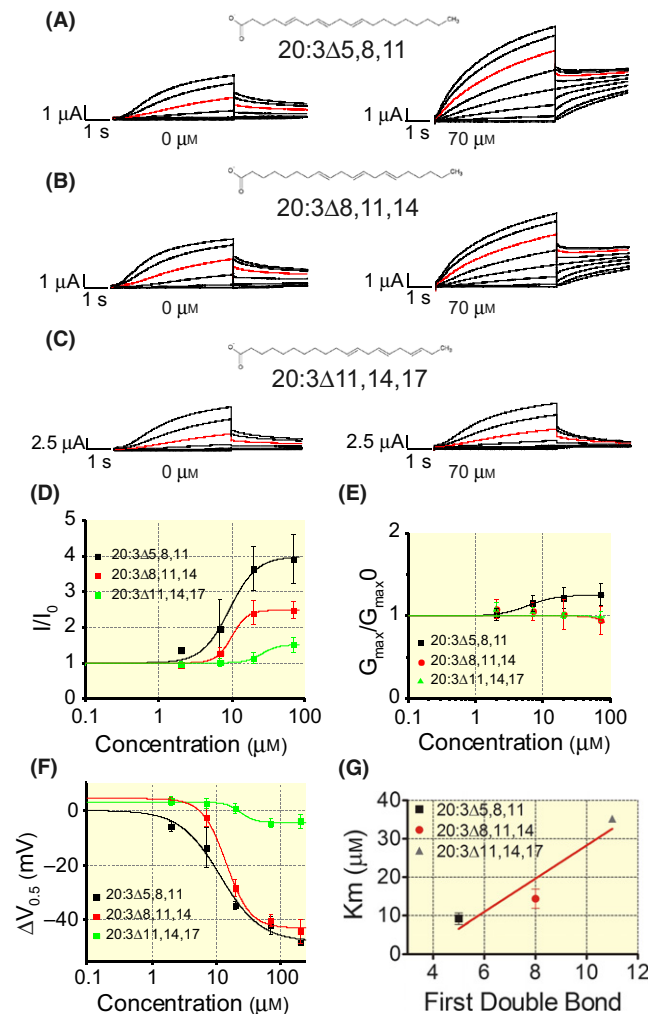


**FIGURE 5** Having a double bond closer to polyunsaturated fatty acid head improves effects on  $I_{K_S}$  channel. A-C,  $K^+$  current in 0  $\mu\text{mol/L}$  (Left) and 70  $\mu\text{mol/L}$  (Right) for (A) 20:3 $\Delta$ 5,8,11, (B) 20:3 $\Delta$ 8,11,14, and (C) 20:3 $\Delta$ 11,14,17. D-F, Comparison of dose dependent (D)  $I/I_0$  increase, (E)  $G_{\text{max}}$  increase, and (F)  $\Delta V_{0.5}$  between 20:3 $\Delta$ 5,8,11, 20:3 $\Delta$ 8,11,14, and 20:3 $\Delta$ 11,14,17. G, Correlation between the position of the first double bond and  $K_m$  of  $I/I_0$  (Slope =  $4.3 \pm 1.5$ ; Adjusted  $R^2 = 0.89$ ;  $P = 0.21$ )

respectively; Figure 6E). In addition, 18:3 $\Delta$ 5,9,12 has the highest apparent affinity ( $6.7 \pm 0.4 \mu\text{mol/L}$ ), whereas 18:3 $\Delta$ 6,9,12 and 18:3 $\Delta$ 9,12,15 exhibited lower apparent binding affinity for  $I/I_0$  ( $10.0 \pm 1.0 \mu\text{mol/L}$  and  $18.7 \pm 0.1 \mu\text{mol/L}$  respectively; Figure 6F). These data further suggest that the location of the first double bond close to the hydrophilic head group of the PUFA was important for improving the effects on and apparent affinity for the  $I_{K_S}$  channel.

To corroborate our conclusion for the importance of the position of the first double bond, we compared three PUFAs (20:3 $\Delta$ 5,8,11, and 22:5 $\Delta$ 4,7,10,13,16, and 18:3 $\Delta$ 5,9,12; Figure 7A-C). These three PUFAs all have the first double bond at positions 4 or 5 but they have

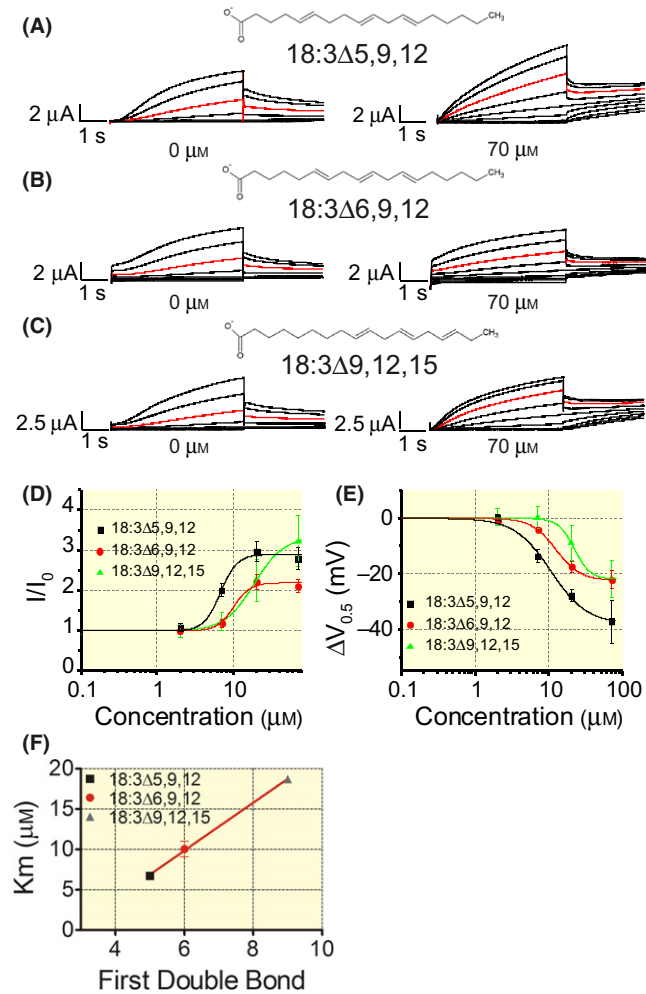


**FIGURE 6** Having the first double bond closer to polyunsaturated fatty acid (PUFA) head in linolenic acid analogues improves PUFA effects on  $I/I_0$  and  $\Delta V_{0.5}$ . A-C,  $K^+$  current in 0 μmol/L (Left) and 70 μmol/L (Right) for (A) 18:3Δ9,12,15, (B) 18:3Δ6,9,12, and (C) 18:3Δ5,9,12. D and E, Comparison of dose dependent (D)  $I/I_0$  increase and (E)  $\Delta V_{0.5}$  between 18:3Δ9,12,15, 18:3Δ6,9,12, and 18:3Δ5,9,12. F, Correlation between the position of the first double bond and  $K_m$  of  $I/I_0$  (Slope =  $3.0 \pm 0.08$ ; Adjusted  $R^2 = 0.99$ ;  $P = 0.02$ )

different carbon tails lengths, a different number of double bonds, and different positions of the other double bonds. The prediction is that PUFAs with the first double bond close to the head group will be similarly effective compounds and have similar apparent affinity for the  $I_{K_s}$  channel. 18:3Δ5,9,12, 22:5Δ4,7,10,13,16, and 20:3Δ5,8,11 all increase the maximum  $I/I_0$  ( $2.9 \pm 0.07$ ,  $3.7 \pm 0.02$ , and  $4.0 \pm 0.23$  respectively; Figure 7D), and  $G_{max}$  ( $1.1 \pm 0.01$ ,  $1.3 \pm 0.02$ , and  $1.3 \pm 0.01$  respectively; Figure 7E), and produce a similar shift in the  $V_{0.5}$  of the  $I_{K_s}$  channel ( $\Delta V_{0.5} = -38 \pm 2.7$  mV,  $-44.4 \pm 10$  mV, and  $-44.7 \pm 4.3$  mV respectively; Figure 7F). 18:3Δ5,9,12, 22:5Δ4,7,10,13,16, and 20:3Δ5,8,11, though they are statistically different in their apparent binding affinities for  $I/I_0$ , ( $K_m = 6.7 \pm 0.4$  μmol/L vs  $3.7 \pm 0.1$ , and  $9.2 \pm 1.4$  μmol/L, respectively; One-way ANOVA  $F$  statistic = 56.3;  $P < 0.001$ ) are all among the PUFAs tested here that have the highest apparent binding affinity for the  $I_{K_s}$  channel.

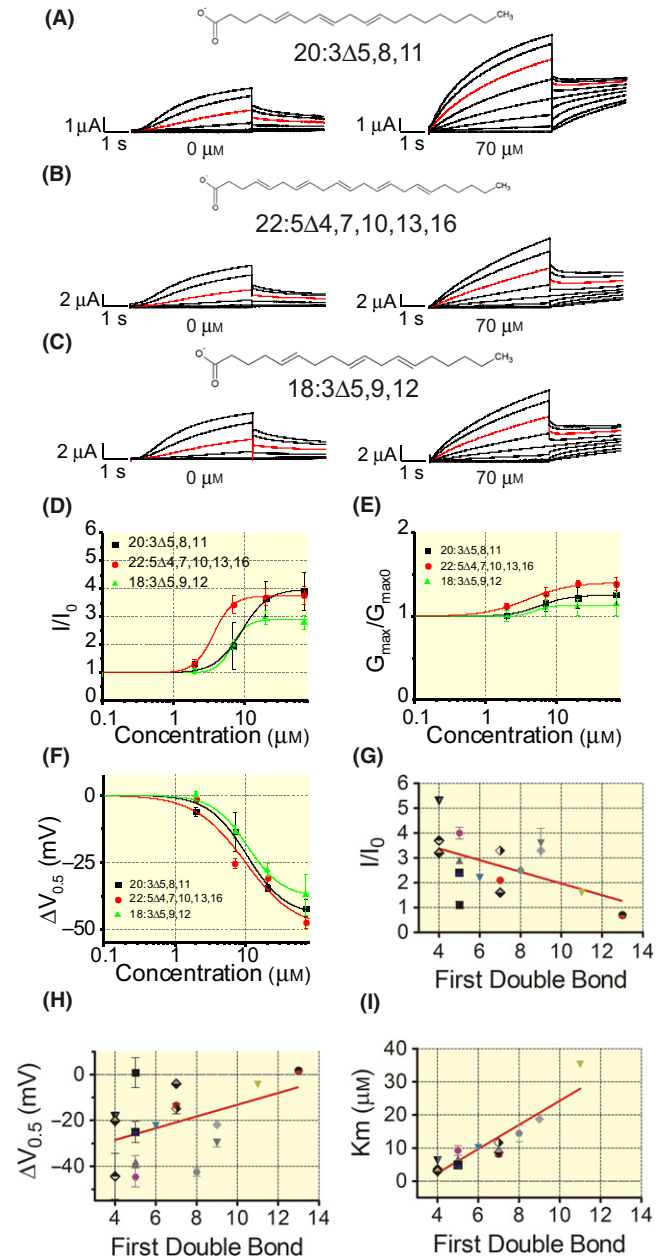


**FIGURE 7** Effects on and affinity for  $I_{K_s}$  channel can be predicted using the position of the first double bond, demonstrated using 18:3Δ5,9,12. A-C,  $K^+$  current in 0 μmol/L (Left) and 70 μmol/L (Right) for (A) 20:3Δ5,8,11, (B) 22:5Δ4,7,10,13,16, and (C) 18:3Δ5,9,12. D-F, Comparison of dose dependent (D)  $I/I_0$  increase, (E)  $G_{max}$ , and (F)  $\Delta V_{0.5}$  between 20:3Δ5,8,11, 22:5Δ4,7,10,13,16, and 18:3Δ5,9,12. G-I, Correlation between the position of the first double bond of all polyunsaturated fatty acids and the (G)  $I/I_0$  (Slope =  $-0.24 \pm 0.1$ ;  $R^2 = 0.27$ ;  $P = 0.04$ ), (H)  $\Delta V_{0.5}$  (Slope =  $2.6 \pm 1.4$ ;  $R^2 = 0.19$ ;  $P = 0.09$ ), and (I)  $K_m$  of  $I/I_0$  (Slope =  $3.6 \pm 0.49$ ;  $R^2 = 0.83$ ;  $P < 0.0001$ )

$I/I_0$ , ( $K_m = 6.7 \pm 0.4$  μmol/L vs  $3.7 \pm 0.1$ , and  $9.2 \pm 1.4$  μmol/L, respectively; One-way ANOVA  $F$  statistic = 56.3;  $P < 0.001$ ) are all among the PUFAs tested here that have the highest apparent binding affinity for the  $I_{K_s}$  channel.



When we compared the effects of all 16 PUFAs tested, there was a significant correlation between the position of the first double bond and  $I/I_0$  (Slope =  $-0.24 \pm 0.1$ ;  $R^2 = 0.27$ ;  $P = 0.04$ ; Figure 7G). There is not a significant correlation between the position of the first double bond and the  $\Delta V_{0.5}$  (Slope =  $2.6 \pm 1.4$ ;  $R^2 = 0.19$ ;  $P = 0.09$ ; Figure 7H). There is no correlation between the position of the first double bond and the maximal conductance ( $G_{\max}$ ; Figure S2D). However, there is a strong and significant correlation between the position of the first double bond relative to the PUFA head and the apparent binding affinity for  $I/I_0$  (double bonds closer to the head group give lower  $K_m$ ; Slope =  $3.6 \pm 0.49$ ;  $R^2 = 0.83$ ;  $P < 0.0001$ ; Figure 7I). These data suggest that the location of the first double bond does indeed contribute to the ability of PUFAs to increase  $K^+$  current with high apparent affinity for the  $I_{Ks}$  channel.

## 2.5 | Hierarchical cluster analysis reveals distinct groupings of PUFAs according to their effects

We grouped PUFAs with similar effects using hierarchical cluster analysis to determine key differences between the PUFAs that were tested.<sup>39</sup> All four effects on the  $I_{Ks}$  channel (ie  $I/I_0$ ,  $\Delta V_{0.5}$ ,  $G_{\max}$ , and  $K_m$  of  $I/I_0$ ) were input simultaneously to be clustered according to similarity in all of the effects. We then looked at the PUFAs that were clustered together to determine whether there are similarities between those PUFAs in their structures (ie tail length, number of double bonds, position of the first double bond, and the position of the last double bond). Our hierarchical cluster analysis revealed three distinct groupings of PUFAs based on dissimilarity of PUFA effects between the groups (denoted by the height of dendrogram branches; Figure 8A). The first grouping (Cluster 1) included 18:3 $\Delta$ 5,9,12, 22:5 $\Delta$ 4,7,10,13,16, 20:3 $\Delta$ 5,8,11, and 20:3 $\Delta$ 8,11,14. All of these PUFAs have their double bonds grouped closer to the PUFA head and they produce the largest left-shifts in the  $V_{0.5}$  of the  $I_{Ks}$  channel. Interestingly, all of these PUFAs are  $\omega$ -6 and  $\omega$ -9 PUFAs. The next grouping (Cluster 2) includes 18:2 $\Delta$ 9,12, 22:4 $\Delta$ 4,10,13,16, 20:5 $\Delta$ 5,8,11,14,17, 22:6 $\Delta$ 4,7,10,13,16,19, and 18:3 $\Delta$ 6,9,12. The following grouping (Cluster 3) includes 18:3 $\Delta$ 9,12,15, 22:5 $\Delta$ 7,10,13,16,19, 16:3 $\Delta$ 7,10,13, and 22:4 $\Delta$ 7,10,13,16. Clusters 2 and 3 both include PUFAs that have moderate effects on the  $I_{Ks}$  channel. The final grouping (Cluster 4) includes 20:3 $\Delta$ 11,14,17, 22:3 $\Delta$ 13,16,19, and 14:3 $\Delta$ 5,8,11, all of which have the majority of their double bonds grouped closer to the end of the PUFA tail and produce little to no change in the  $V_{0.5}$  of the  $I_{Ks}$  channel. Interestingly, all of these PUFAs are  $\omega$ -3 PUFAs. Clusters 1 and 4 demonstrated the greatest dissimilarity in their effects. The hierarchical cluster analysis

suggests that the PUFAs with double bonds located closer to the PUFA head (Cluster 1) resulted in the greatest left-shift in the  $V_{0.5}$ . In addition, the PUFAs with double bonds further from the PUFA head (Cluster 4) produced the smallest changes in the  $V_{0.5}$ , which is in line with our single variable regression analysis and conclusions. Most PUFAs in Clusters 2 and 3 were either  $\omega$ -3 PUFAs with a double bond close to the head group or  $\omega$ -6 PUFAs with no double bond close to the head group. These PUFAs had intermediate effects on the  $I_{Ks}$  channel. The pattern that emerges from this analysis is that the most effective PUFAs on the  $I_{Ks}$  channel are PUFAs with a double bond close to the head group (position 4 or 5), but that lack a double bond close to the end of the PUFA tail ( $\omega$ -6 and  $\omega$ -9 PUFAs). For example, when the first and last double bonds are both shifted closer to the end of the tail (ie

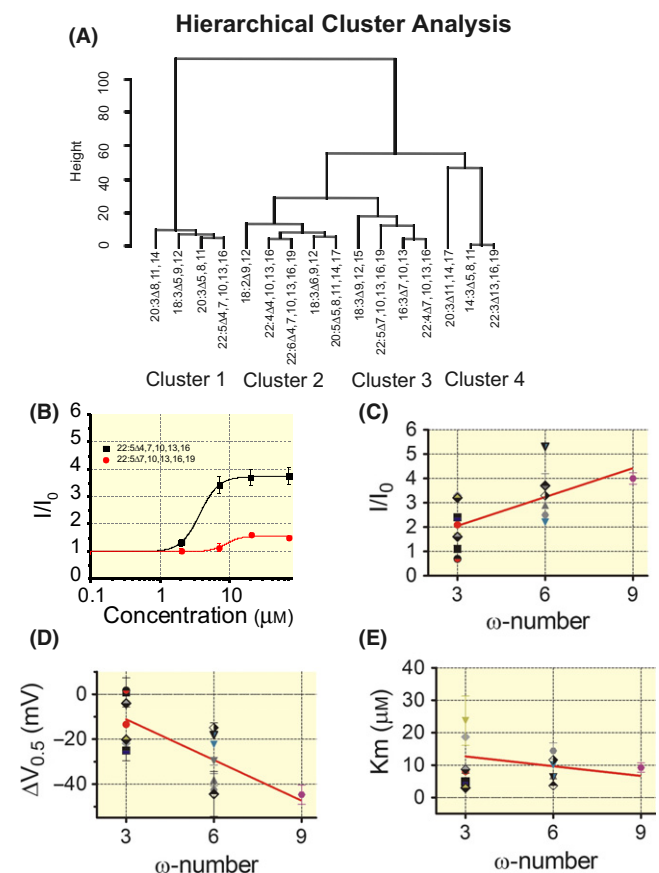


**FIGURE 8** Hierarchical clustering suggests three distinct groups of polyunsaturated fatty acids (PUFAs) and suggests role of  $\omega$ -number in effects on  $I_{Ks}$ . A, Dendrogram of all PUFAs tested grouped according to their effects on the  $I_{Ks}$  channel. B, Comparison of dose dependent  $I/I_0$  increase between 22:5 $\Delta$ 4,7,10,13,16 (Cluster 1) and 22:5 $\Delta$ 7,10,13,16,19 (Cluster 3). C-E, Correlation between the position of the last double bond of all PUFAs and (C)  $I/I_0$  (Slope =  $0.39 \pm 0.13$ ;  $R^2 = 0.40$ ;  $P = 0.009$ ), (D)  $\Delta V_{0.5}$  (Slope =  $-6.0 \pm 1.5$ ;  $R^2 = 0.54$ ;  $p = 0.001$ ), and (E)  $K_m$  of  $I/I_0$  (Slope =  $-1.0 \pm 1.3$ ;  $R^2 = 0.05$ ;  $P = 0.45$ )

shifted closer to the omega carbon) by comparing 22:5Δ4,7,10,13,16 (Cluster 1) to 22:5Δ7,10,13,16,19 (Cluster 3) the  $I_{I_0}$  is reduced by nearly half. (Figure 8B). Because the cluster analysis suggests that the ω-6 and ω-9 PUFAs produce the largest shifts in the  $V_{0.5}$ , we correlate the ω-number with each of the effects on the  $I_{K_s}$  channel. There is a significant correlation between the ω-number and  $I_{I_0}$  (Slope =  $0.39 \pm 0.13$ ;  $R^2 = 0.40$ ;  $P = 0.009$ ; Figure 8C). In addition, there is a strong correlation between ω-number and the  $\Delta V_{0.5}$ , which is consistent with our findings from the dendrogram grouping (Slope =  $-6.0 \pm 1.5$ ;  $R^2 = 0.54$ ;  $P = 0.001$ ; Figure 8D). However, there is no correlation between the ω-number and the maximal conductance ( $G_{max}$ ; Figure S2E). There is also no correlation between the ω-number and apparent binding affinity (Slope =  $-1.0 \pm 1.3$ ;  $R^2 = 0.05$ ;  $P = 0.45$ ; Figure 8E).

## 2.6 | Multivariable regression analysis

To test whether the PUFA effects —  $I_{I_0}$ ,  $\Delta V_{0.5}$ ,  $G_{max}$ , and  $K_m$  of  $I_{I_0}$  — depend on a combination of the different parameters (Length, number of double bonds, and location of the first and last double bonds) of the PUFA tails, we conducted a multivariable regression of each PUFA effect using combinations of the four PUFA parameters simultaneously (Figure S3). The multivariable regression using all four parameters improved the fit for  $I_{I_0}$  (Adjusted  $R^2$  increased from 0.40 to 0.54) and  $G_{max}$  (Adjusted  $R^2$  increased from 0.25 to 0.60). According to the multivariable regression analysis  $I_{I_0}$  is significantly correlated to the location of the first double bond (Table 2).  $G_{max}$  is significantly correlated to the length of the tail, the number of double bonds and the location of the first and last double bond (Table 2). However, the  $\Delta V_{0.5}$  and  $K_m$  (for  $I_{I_0}$ ) single regressions were not improved by the addition of more

parameters of the PUFA. This suggests that the  $\Delta V_{0.5}$  and  $K_m$  (for  $I_{I_0}$ ) are highly dependent on single PUFA parameters (ie the position of the last double bond and first double bond respectively). To show the quality of the fit of the multivariable analysis, we show in Figure S3 the measured and the predicted values for the fits of  $I_{I_0}$  (Figure S3A) and  $G_{max}$  (Figure S3B).

## 3 | DISCUSSION

Neither the length of the carbon tail nor the number of double bonds in the tail showed a strong correlation with the effects on the  $I_{K_s}$  currents or the affinity for the  $I_{K_s}$  channel. However, there were correlations between having the first double bond closer to the PUFA head and increasing  $I_{I_0}$  and improving the apparent binding affinity for  $I_{I_0}$  (lower  $K_m$ ). In contrast, having a double bond close to the end of the PUFA tail (ie an ω-3 PUFA) decreased the effect of the PUFA on the  $V_{0.5}$  of the  $I_{K_s}$  channel, whereas having a double bond further away from the end of the PUFA tail (ie an ω-6 or ω-9 PUFA) increases the effect of the PUFA on the  $V_{0.5}$ . Using our data, the location of the first and the last double bonds, relative to the PUFA head can therefore be used to develop effective PUFAs that bind with high affinity to the  $I_{K_s}$  channel.

One of the main obstacles to the clinical use of PUFAs for cardiovascular diseases has been inconsistencies in clinical trials investigating the relationship between dietary fatty acids and cardiovascular disease risk. Two recent clinical studies report on correlation between ω-3 and ω-6 fatty acid supplements with cardiovascular disease risk.<sup>40,41</sup> In a meta-analysis of 10 clinical trials looking at the relationship between ω-3 fatty acid supplements and the risk for cardiovascular disease and negative disease outcomes, Aung et al,<sup>40</sup> reported that there is no significant correlation between the use of ω-3 fatty acid supplements and cardiovascular disease risk. In contrast, Virtanen et al<sup>41</sup> reported beneficial effects of ω-6 PUFAs on cardiovascular disease risk in the Kuopio Ischaemic Heart Disease Risk Factor Study. These findings are in agreement with our conclusions that ω-3 PUFAs have reduced left-shifting effects on the  $I_{K_s}$  voltage dependence whereas ω-6 PUFAs (along with ω-9 PUFAs) are the most beneficial for left-shifting the  $I_{K_s}$  voltage dependence and increasing  $I_{K_s}$  current.

Tian et al,<sup>42</sup> applied PUFAs, such as DHA (22:6Δ4,7,10,13,16,19), onto Slo1-β1 BK channels to determine the important features for PUFAs to interact with BK channels. They concluded that double bonds at least halfway through the PUFA tail (at carbons 9-12) are important for a high affinity interaction of PUFAs with Slo1 BK channels. They proposed that these double bonds

**TABLE 2** Multiple regression analysis results

Variables	$I_{I_0}$	$G_{max}$
$C_L$	$0.62 \pm 0.29$ ns	$0.39 \pm 0.09$ ***
$C_{\#B}$	$-1.6 \pm 0.87$ ns	$-0.97 \pm 0.27$ **
$C_{FB}$	$-0.65 \pm 0.28$ *	$-0.34 \pm 0.09$ **
$C_{LB}$	$-0.26 \pm 0.33$ ns	$-0.33 \pm 0.10$ **
$C_0$	2.7	1.22
Adj. $R^2$	0.54	0.6
$F$	0.01	0.005

The measured outcomes ( $I_{I_0}$  and  $G_{max}$ ) were fitted to the equation  $y = C_0 + C_L \times (\text{Tail length} - \text{Average Tail Length}) + C_{\#B} \times (\text{Number of double bonds} - \text{Average number of double bonds}) + C_{FB} \times (\text{Position of the first double bond} - \text{Average position of the first double bond}) + C_{LB} \times (\omega\text{-number} - \text{Average } \omega\text{-number})$ .  $C_0$  is the average response of all tested PUFAs. \* $P < 0.05$ , \*\* $P < 0.01$ , \*\*\* $P < 0.001$ , ns = not significant.

allow more curvature of the PUFA molecule and make it more compact, thus increasing the stability of the PUFA in its binding site.<sup>42</sup> In contrast, we find here that the double bonds closer to the PUFA head groups (at carbons 4-5) are important for the effect on and apparent binding affinity for the  $I_{Ks}$  channel. However, how the PUFA tail specifically interacts with the  $I_{Ks}$  channel to increase the apparent binding affinity is not known from this data and will be the focus of future studies.

Tian et al,<sup>42</sup> proposed that the PUFA head group takes part in an anion- $\pi$  interaction with a tyrosine residue in the S6 segment of Slo1 BK channels. In contrast, we previously showed that the effects on the  $I_{Ks}$  channel are mainly due to an electrostatic interaction between the PUFA head group and the positively charged S4 segment of the  $I_{Ks}$  channel.<sup>12</sup> PUFA effects on the BK channels are believed to be due to PUFAs in the inner leaflet of the membrane, whereas our effects on  $I_{Ks}$  channels are believed to be due to PUFAs in the outer leaflet of the membrane. This fact, along with their different putative site of DHA interaction, is indicative of different mechanisms for the PUFA effects on BK and  $I_{Ks}$  channels (intracellular action on S6 vs extracellular action on S4). Different mechanisms for PUFA effects on various ion channels is also supported by the effects of PUFAs on cardiac  $Na^+$  and  $Ca^{2+}$  channels. For example, in contrast to the increase in currents shown here for DHA and Eicosapentaenoic acid (EPA) on  $I_{Ks}$  channels, DHA and EPA have been shown to reduce the currents through voltage-gated  $Na^+$  and  $Ca^{2+}$  channels.<sup>31,33,35</sup> This further suggests different mechanisms of action of PUFAs on different voltage-gated ion channels. Therefore, there is a possibility for channel-specific PUFA interactions which could be, in part, attributed to different features of the PUFA tail. Future studies would have to determine what PUFA features are important for other cardiac ion channels and whether channel-specific PUFAs could be developed.

Our current model for how PUFAs affect the  $I_{Ks}$  channel is that (a) the PUFA tail inserts into the lipid bilayer, (b) the PUFA then diffuses in the membrane to the  $I_{Ks}$  channel, (c) the PUFA tail binds to the  $I_{Ks}$  channel and anchors the PUFA head group near the positively charged voltage sensor of the  $I_{Ks}$  channel, (d) the negatively charged head group of the PUFA electrostatically attracts the voltage sensor and activates the  $I_{Ks}$  channel.<sup>12</sup> The presently reported changes in the apparent PUFA affinity for the  $I_{Ks}$  channel due to variations in the PUFA tail are consistent with this model. However, in addition to changing the apparent PUFA affinity to the  $I_{Ks}$  channel, we here show that the positions of the double bonds of the PUFAs also affects the size of the left-shift of the voltage dependence of the  $I_{Ks}$  channel (eg the position of the last double bond in the tail) and, in some instances, also affects the

maximal conductance of the  $I_{Ks}$  channel. The reasons for these additional effects are not clear. It is possible that the interactions between the last double bonds and the  $I_{Ks}$  channel alter the location of the negatively charged head group of the PUFAs relative to the charges in S4 and thereby cause bigger or smaller shifts in the voltage dependence of activation.

The PUFAs were tested at pH 9, a pH at which the carboxyl head group of the PUFA molecules interacting with the  $I_{Ks}$  channel are expected to be deprotonated and negatively charged, with no additional effects on normal wild type  $I_{Ks}$  function compared to pH 7.5 (Figure S4). Our group has previously described that DHA (22:6 $\Delta$ 4,7,10,13,16,19) increases Kv7.1  $K^+$  current at pH 7.5, but that this effect is abolished when Kv7.1 is co-expressed with the accessory  $\beta$ -subunit KCNE1.<sup>12</sup> The head groups of N-AT and DHA-glycine are more efficacious than DHA on  $I_{Ks}$  channels, because they remain more deprotonated and negatively charged at physiological pH 7.5. Knowing that a PUFA head with a lower pKa increases  $I_{Ks}$  current at physiological pH = 7.5, we can now begin making modifications in the tails of these PUFA analogues to improve the binding affinity to the  $I_{Ks}$  channel based on the data reported here. Understanding the role of the double bonds for the PUFA tail in altering the binding affinity to the  $I_{Ks}$  channel will allow us to develop new PUFA analogues with better effect on  $I_{Ks}$  channels by attaching high affinity tails to head groups, such as taurine or glycine, that are more deprotonated and efficacious at physiological pH.

The work presented here was performed using the *X. laevis* oocytes expression system. This poses some limitations to understanding the effects of PUFAs on the physiological  $I_{Ks}$  channel due to the absence of intrinsic factors in human cardiomyocytes that can influence the  $I_{Ks}$  macromolecular complex. Ongoing and future experiments will determine the effects of the PUFAs examined here on the  $I_{Ks}$  current present in human cardiomyocytes to further understand the therapeutic potential of PUFAs as anti-arrhythmic compounds. In addition, our experiments only shed light on the acute effects of PUFAs applied to the  $I_{Ks}$  channel. Further experiments are needed to determine the long-term effects of chronic application of PUFAs to the  $I_{Ks}$  channel.

The next step in understanding the important properties of PUFAs for increasing  $I_{Ks}$  current in LQTS is to test whether the PUFAs deemed effective here on wild type  $I_{Ks}$  channels are able to reverse Long QT mutation phenotypes in  $I_{Ks}$  channels. Mutations in the  $I_{Ks}$  channel that cause LQTS type 1 (LQT1) cause loss-of-function in the  $I_{Ks}$  channel by a variety of mechanisms, including a right-shift in the voltage dependence of the  $I_{Ks}$  channel, changes in channel kinetics or alterations in trafficking to the cell

membrane.<sup>9,13,43</sup> Here, we showed that  $\omega$ -6 (and  $\omega$ -9) PUFAs with double bonds close to the PUFA head produce the largest increases in  $K^+$  current, shift the wild type G-V curve leftward the most, and activate the channel at more negative voltages. These data suggest that applying the same PUFAs to a mutated  $I_{Ks}$  channel would restore the wild type  $I_{Ks}$  current and, therefore, restore the normal ventricular action potential. A previous study from our group showed that a modified PUFA, N-arachidonoyl taurine (N-AT), could restore much of the defects of eight different LQTS-causing mutations, albeit at high N-AT concentrations.<sup>13</sup> This presents a need for new PUFA analogues that can influence  $I_{Ks}$  currents in a lower concentration range which would be more therapeutically relevant and reduce potential side effects on other channels. The findings reported here provide a foundation for the design of higher affinity PUFA analogues that can be used for the treatment of LQTS. Future experiments need to be done to test the best compounds found here on  $I_{Ks}$  channels bearing LQT1-causing mutations. In addition, because different PUFAs shift the G-V curve by different amounts and different LQT1 mutations shift the G-V curves by different amounts in the opposite direction along the voltage axis, one could develop mutation-specific therapeutics by matching each PUFA with each mutation depending on their relative effects on the G-V curves.

## 4 | MATERIALS AND METHODS

### 4.1 | Molecular biology

Kv7.1 and KCNE1 channel cRNA were transcribed using the mMACHINE mMESSAGE T7 kit (Ambion, Foster City, CA, USA). Fifty nanograms of cRNA were injected at a 3:1, weight:weight (Kv7.1:KCNE1) ratio into defolliculated *X. laevis* oocytes (Ecocyte, Austin, TX, USA) for  $I_{Ks}$  channel expression. Injected cells were incubated for 72-96 h in standard ND96 solution (96 mmol/L NaCl, 2 mmol/L KCl, 1 mmol/L MgCl<sub>2</sub>, 1.8 mmol/L CaCl<sub>2</sub>, 5 mmol/L HEPES; pH = 7.5) containing 1 mmol/L pyruvate at 16°C prior to electrophysiological recordings.

### 4.2 | Two-electrode voltage clamp

*Xenopus laevis* oocytes, co-expressing wild type Kv7.1 and KCNE1, were recorded in the two-electrode voltage clamp (TEVC) configuration. Recording pipettes were filled with 3 mol/L KCl. The recording chamber was filled with ND96 (96 mmol/L NaCl, 2 mmol/L KCl, 1 mmol/L MgCl<sub>2</sub>, 1.8 mmol/L CaCl<sub>2</sub>, 5 mmol/L Tricine; pH 9). PUFAs were obtained from Cayman Chemical (Ann Arbor, MI, USA) or Larodan (Solna, Sweden) and kept at -20°C as 100 mmol/L stock solutions in ethanol. Serial dilutions

of the different PUFAs were prepared from stocks to make 2, 7, 20 and 70  $\mu$ mol/L concentrations in ND96 solutions (pH = 9.0). PUFAs were perfused into the recording chamber using the Rainin Dynamax Peristaltic Pump (Model RP-1; Rainin Instrument, Oakland, CA, USA, San Jose, CA, USA). Electrophysiological recordings were obtained using Clampex 10.3 software (Axon, pClamp; Molecular Devices, San Jose, CA, USA). During the application of PUFAs the membrane potential was stepped every 30 seconds from -80 to 0 mV for 5 seconds before stepping to -40 mV and back to -80 mV to ensure that the PUFA effects on the current at 0 mV reached steady state (Figure 1D). A voltage-step protocol was used to measure the current vs voltage (I-V) relationship before PUFA application and after the PUFA effects had reached steady state for each concentration of PUFA. Cells were held at -80 mV followed by a hyperpolarizing prepulse to -140 mV to make sure all channels are fully closed. The voltage was then stepped from -100 to 60 mV (in 20 mV steps) followed by a subsequent voltage step to -20 mV to measure tail currents before returning to the -80 mV holding potential (Figure 1A).

### 4.3 | Data analysis

Tail currents (measured at arrows in Figure 1A,B) were analysed using Clampfit 10.3 software in order to obtain conductance vs voltage (G-V) curves to determine the voltage dependence of channel activation. The  $V_{0.5}$ , the voltage at which half the maximal current occurs, was obtained by fitting the G-V curves from each concentration of PUFA with a Boltzmann equation (Figure 1C):

$$G(V) = \frac{G_{\max}}{1 + e^{(V_{0.5}-V)/s}} \quad (1)$$

where  $G_{\max}$  is the maximal conductance at positive voltages and  $s$  is the slope factor in mV. The current values for each concentration at 0 mV ( $I/I_0$ , arrow in Figure 1C) were used to plot the dose response curves for each PUFA (Figure 1E). These dose response curves were fit using the Hill equation in order to obtain the  $K_m$  value for each PUFA (Figure 1E):

$$\frac{I}{I_0} = 1 + \frac{A}{1 + \frac{K_m^n}{x^n}} \quad (2)$$

where  $A$  is the fold increase in current caused by the PUFA at saturating concentrations,  $K_m$  is the apparent affinity of the PUFA,  $x$  is the concentration, and  $n$  is the Hill coefficient. Fitted maximum values derived from the dose response curves are reported for each of the effects ( $I/I_0$ ,  $\Delta V_{0.5}$ , and  $G_{\max}$ ) from the different PUFAs tested. In some cases, there is variability in the  $V_{0.5}$  in the control solution (i.e. 0 PUFA) between batches of oocytes. In order to correct for variability due to oocytes, when the

$V_{0.5}$  in the control solution was greatly different than 20 mV, we applied a correction in order to more accurately measure PUFA-induced  $I_{Ks}$  current increases. We subtracted the  $V_{0.5}$  (given by fitting the G-V with a Boltzmann equation) by 20 mV and used the current measured at the resulting voltage. The maximum conductance ( $G_{max}$ ) was calculated by taking the difference between the maximum and minimum current values (using the G-V curve for each concentration) and then normalizing to control solution (0  $\mu$ mol/L). Graphs plotting mean and standard error of the mean (SEM) for  $I/I_0$ ,  $\Delta V_{0.5}$ ,  $G_{max}$ , and  $K_m$  were generated using the Origin 9 software (Northampton, MA, USA).

Hierarchical cluster analysis was conducted using R-based clustering software.<sup>39</sup> Input data for each PUFA were numerical values for mean  $I/I_0$ ,  $\Delta V_{0.5}$ ,  $G_{max}$ , and  $K_m$ . The height of the dendrogram branches represent the dissimilarity between the clusters. Longer branches between nodes connecting clusters indicate that those clusters exhibit very different effects on the  $I_{Ks}$  channel. The PUFAs that are clustered together as a result of the hierarchical cluster analysis are therefore the most similar in their effects on the  $I_{Ks}$  channel.

#### 4.4 | Statistics

Single and multivariable regression statistics were computed using GRAPHPAD PRISM (GraphPad Software, La Jolla, CA, USA) and Origin 9 software respectively. We conducted single linear regression on each of the PUFA parameters with each of the effects we were interested in (ie  $I/I_0$ ,  $V_{0.5}$ ,  $G_{max}$ , and  $K_m$ ) to determine the slope of the fit, the adjusted  $R^2$ , and  $t$ -values. In addition, we conducted multivariable regression for all of the PUFA parameters simultaneously with each of the effects to determine again the slope, the adjusted  $R^2$ , and  $F$ -values. Results were considered significant if  $P < 0.05$ .

#### ACKNOWLEDGMENTS

We thank Dr. Rene Barro-Soria and Dr. Fredrik Elinder for helpful feedback on the manuscript. We also thank Thea Wennman, Amanda Dahl, Johanna Nilsen, and Amanda Wessne for their contributions to experiments during their time as visiting scholars.


#### CONFLICT OF INTEREST

SIL, HPL: A patent application (62/032,739) has been submitted by the University of Miami with SIL and HPL as inventors. The other authors declare no other competing interests.

#### AUTHOR CONTRIBUTIONS

BMB, Analysis, and interpretation of data, Drafting or revising the article; MEP, Acquisition of data; SIL, Conception and design, Acquisition of data, Drafting or revising the article; HPL, Conception and design, Analysis and interpretation of data, Drafting or revising the article.

#### ORCID

Briana M. Bohannon  <http://orcid.org/0000-0002-3720-1477>  
Sara I. Liin  <http://orcid.org/0000-0001-8493-0114>  
Hans Peter Larsson  <http://orcid.org/0000-0002-1688-2525>

#### REFERENCES

- Hille B. *Ion Channels of Excitable Membranes*. Sunderland, MA: Sinauer Associates; 2001.
- Deal KK, England SK, Tamkun MM. Molecular physiology and cardiac potassium channels. *Physiol Rev*. 1996;76(1):49-67.
- Salata JJ, Jurkiewicz NK, Jow B, et al.  $I_K$  of rabbit ventricle is composed of two currents: evidence for  $I_{Ks}$ . *Am J Physiol*. 1996;271:H2477-H2488.
- Lei M, Brown HF. Two components of the delayed rectifier potassium current,  $I_K$ , in rabbit sino-atrial node cells. *Exp Physiol*. 1996;81:725-740.
- Li GR, Feng J, Yue L, Carrier M, Nattel S. Evidence for two components of delayed rectifier  $K^+$  current in human ventricular myocytes. *Circ Res*. 1996;78(4):689-695.
- Veldkamp MW, Van Ginneken ACG, Opthof T, Bouman LN. Delayed rectifier channels in human ventricular myocytes. *Circulation*. 1995;92(12):3497-3503.
- Noble D, Tsien RW. Reconstruction of the repolarization process in cardiac Purkinje fibres based on voltage clamp measurements of membrane current. *J Physiol*. 1969;200:233-254.
- Noble D, Tsien RW. Outward membrane currents activated in the plateau range of potentials in cardiac Purkinje fibres. *J Physiol*. 1969;200:205-231.
- Bohnen MS, Peng G, Robey SH, et al. Molecular pathophysiology of congenital Long QT Syndrome. *Physiol Rev*. 2017;97:89-134.
- Mohrman DE, Heller LJ. *Cardiovascular Physiology*, 7th edn. New York, NY: McGraw Hill; 2010.
- Sanguinetti M. Dysfunction of delayed rectifier potassium channels in an inherited cardiac arrhythmia. *Ann N Y Acad Sci*. 1999;868:406-412.
- Liin SI, Ejneby MS, Barro-Soria R, et al. Polyunsaturated fatty acid analogs act antiarrhythmically on the cardiac  $I_{Ks}$  channel. *Proc Natl Acad Sci USA*. 2015;112(18):5714-5719.
- Liin SI, Larsson JE, Barro-Soria R, Bentzen BH, Larsson HP. Fatty acid analogue N-arachidonoyl taurine restores function of  $I_{Ks}$  channels with diverse long QT mutations. *Elife*. 2016;5:e20272.
- Panaghie G, Tai KK, Abbott GW. Interaction of KCNE subunits with the KCNQ1  $K^+$  channel pore. *J Physiol*. 2006;570:455-466.
- Sanguinetti M, Curran ME, Zou A, et al. Coassembly of KvLQT1 and minK (IsK) proteins to form cardiac  $I_{Ks}$  potassium channel. *Nature*. 1996;384:80-83.

16. Barhanin J, Lesage F, Guillemare E, Fink M, Lazdunski M, Romey G. KvLQT1 and Isk (minK) proteins associate to form the  $I_{Ks}$  cardiac potassium current. *Nature*. 1996;384:78-80.
17. Sun J, MacKinnon R. Cryo-EM structure of a KCNQ1/CaM complex reveals insights into congenital Long QT Syndrome. *Cell*. 2017;169:1042-1059.
18. Peroz D, Rodriguez N, Choveau F, Baro I, Merot J, Loussouam G. Kv7.1 (KCNQ1) properties and channelopathies. *J Physiol*. 2008;586:1785-1789.
19. Liin SI, Barro-Soria R, Larsson HP. The KCNQ1 channel-remarkable flexibility in gating allows for functional versatility. *J Physiol*. 2015;593:2605-2615.
20. Borjesson SI, Elinder F. Structure, function, and modification of the voltage sensor in voltage-gated ion channels. *Cell Biochem Biophys*. 2008;52:149-174.
21. Larsson HP, Baker OS, Dhillon DS, Isacoff EY. Transmembrane movement of the shaker  $K^+$  channel S4. *Neuron*. 1996;16:387-397.
22. Bezanilla F. How membrane proteins sense voltage. *Nat Rev*. 2008;9:323-332.
23. Chen H, Goldstein SAN. Serial perturbation of MinK in  $I_{Ks}$  implies an  $\alpha$ -helical transmembrane span traversing the channel corpus. *Biophys J*. 2007;93:2332-2339.
24. Gofman Y, Shats S, Attali B, Haliloglu T, Ben-Tal N. How does KCNE1 regulate the Kv7.1 potassium channel? Model-structure, mutations, and dynamics of the Kv7.1-KCNE1 complex. *Structure*. 2012;20:1343-1352.
25. Murray CI, Westhoff M, Eldstrom J, Thompson E, Emes R, Fedida D. Unnatural amino acid photo-crosslinking of the  $I_{Ks}$  channel complex demonstrates a KCNE1:KCNQ1 stoichiometry of up to 4:4. *Elife*. 2016;5:e11815.
26. Barro-Soria R, Rebolledo S, Liin SI, et al. KCNE1 divides the voltage-sensor movement in KCNQ1/KCNE1 channels into two steps. *Nat Commun*. 2014;5:3750-3761.
27. Yang Y, Sigworth F. Single-channel properties of  $I_{Ks}$  potassium channels. *J Gen Physiol*. 1998;112:665-678.
28. Alders M, Bikker H, Christiaans I. Long QT Syndrome. In: Adam MP, Ardinger HH, Pagon RA, et al., eds. *GeneReviews*® [Internet]. Seattle, WA: University of Washington; 2003:1993-2017.
29. Cho Y. Management of patients with Long QT Syndrome. *Korean Circ J*. 2016;46(6):5.
30. Benatti P, Peluso G, Nicolai R, Calvani M. Polyunsaturated fatty acids: biochemical, nutritional, and epigenetic properties. *J Am Coll Nutr*. 2004;23:281-302.
31. Kang J, Leaf A. Evidence that free polyunsaturated fatty acids modify  $Na^+$  channels by directly binding to the channel proteins. *Proc Natl Acad Sci USA*. 1996;93:3542-3546.
32. Kang J, Leaf A. Prevention of fatal cardiac arrhythmias by polyunsaturated fatty acids. *Am J Clin Nutr*. 2000;71:6.
33. Xiao YF, Kang JX, Morgan JP, Leaf A. Blocking effects of polyunsaturated fatty acids on  $Na^+$  channels of neonatal rat cardiomyocytes. *Proc Natl Acad Sci USA*. 1995;92:11000-11004.
34. Xiao YF, Qingen K, Wang SY, et al. Single point mutations affect fatty acid block of human myocardial sodium channel  $\alpha$  subunit  $Na^+$  channels. *Proc Natl Acad Sci USA*. 2001;98(6):3606-3611.
35. Xiao YF, Gomez AM, Morgan JP, Lederer WJ, Leaf A. Suppression of voltage-gated L-type  $Ca^{2+}$  currents by polyunsaturated fatty acids in adult and neonatal rat ventricular myocytes. *Proc Natl Acad Sci USA*. 1997;94:4182-4187.
36. Borjesson SI, Hammarstrom S, Elinder F. Lipoelectric modification of ion channel voltage gating by polyunsaturated fatty acids. *Biophys J*. 2008;95:2242-2252.
37. Borjesson S, Elinder F. An electrostatic potassium channel opener targeting the final voltage sensor transition. *J Gen Physiol*. 2011;137(6):15.
38. O'Hara T, Virag L, Varro A, Rudy Y. Simulation of the undiseased human cardiac ventricular action potential: model formulation and experimental validation. *PLoS Comput Biol*. 2011;7(5):29.
39. Wessa P. Hierarchical clustering (v1.0.5) in free statistics software (v1.2.1). 2017.
40. Aung T, Halsey J, Kromhout D, et al. Associations of omega-3 fatty acid supplement use with cardiovascular disease risks: meta-analysis of 10 trials involving 77917 individuals. *JAMA Cardiol*. 2018;3:9.
41. Virtanen JK, Wu JHY, Voutilainen S, Mursu J, Tuomainen TP. Serum n-6 polyunsaturated fatty acids and risk of death: the Kuopio Ischaemic Heart Disease Risk Factor Study. *Am J Clin Nutr*. 2018;107:8.
42. Tian Y, Aursnes M, Hansen TV, et al. Atomic determinants of BK channel activation by polyunsaturated fatty acids. *Proc Natl Acad Sci USA*. 2016;113:13905-13937.
43. Huang H, Kuenze G, Smith J, et al. Mechanisms of KCNQ1 channel dysfunction in Long QT Syndrome involving voltage sensor domain mutations. *Sci Adv*. 2018;4:13.

## SUPPORTING INFORMATION

Additional supporting information may be found online in the Supporting Information section at the end of the article.

**How to cite this article:** Bohannon BM, Perez ME, Liin SI, Larsson HP.  $\omega$ -6 and  $\omega$ -9 polyunsaturated fatty acids with double bonds near the carboxyl head have the highest affinity and largest effects on the cardiac  $I_{Ks}$  potassium channel. *Acta Physiol*. 2019;225:e13186. <https://doi.org/10.1111/apha.13186>